Combination of in vitro thermally-accelerated ageing and Fourier-Transform Infrared spectroscopy to predict scaffold lifetime

Credson Langueh, Sylvie Changotade, Salah Ramtani, Didier Lutomski, Géraldine Rohman

Version of Record: https://www.sciencedirect.com/science/article/pii/S0141391020303839
Manuscript_71bb1ed344515c8836c1fb37ee0234bf

Combination of *in vitro* thermally-accelerated ageing and Fourier-Transform Infrared spectroscopy to predict scaffold lifetime

Suggestion for an abbreviated running title: **Accelerated ageing and FTIR spectroscopy to predict scaffold lifetime**

Credson Langueh[a], Sylvie Changotade[a], Salah Ramtani[b], Didier Lutomski[a], Géraldine Rohman[a,*]

[a]Université Sorbonne Paris Nord, URB2I, UR 4462, F-93000, Bobigny, France, Université de Paris, F-92049, Montrouge, France

[b]Université Sorbonne Paris Nord, CSPBAT, UMR CNRS 7244, F-93430, Villetaneuse, France

***Corresponding author:**

Dr Géraldine Rohman

URB2I UR 4462

Université Sorbonne Paris Nord - UFR SMBH

74 rue Marcel Cachin

93000 Bobigny, France

Phone: +33 1 48 38 88 83

EMail: geraldine.rohman@univ-paris13.fr

Abstract

Biodegradable elastomers face a growing use in soft tissue engineering due to the possibility to tune, by an appropriate selection of the synthesis and process conditions, the material thermo-mechanical properties to match the stress–strain behavior of the tissue to replace. However, changes in material properties can impact drastically the scaffold durability and therefore the efficiency of tissue reconstruction. Few studies focus on approaches allowing the prediction of the scaffold lifetime, while there is a need for strategies using accelerated testing protocols and versatile tools to easily investigate on the material degradation rate.

In the present study, elastomeric cross-linked poly(ester-urethane-urea) scaffolds have been developed through an emulsion technique allowing to produce highly interconnected porous structure. Thermally-accelerated ageing was performed in cell culture medium at different temperatures: 37°C, 55°C, 75°C and 90°C. The degradation process was followed by gravimetry, swelling measurements, compression tests and infrared spectroscopy. The study revealed that the scaffold chemical composition variation was temperature dependant and its analysis by Fourier-Transform infrared spectroscopy allowed an easy determination of the activation energy of the hydrolytic degradation process, leading to the prediction of the scaffold lifetime at 37°C using Arrhenius extrapolation. This approach could be used to simply and straightforwardly screen the durability of new scaffolds.

Keywords: FTIR spectroscopy; scaffold; accelerated ageing; lifetime; activation energy

1. Introduction

In tissue engineering, the challenging goal is the elaboration of appropriate porous scaffolds that could allow, among others, cell adhesion to the pore surface, cell migration within the porous structure, three-dimensional tissue development, maturation and vascularization [1]. As a consequence, some requirements that the scaffold must possess have been identified, such as porosity, pore size, chemical composition and wettability, and must be adapted to targeted cells and tissues to replace. These properties are continuously optimized to improve tissue regeneration rate and quality but impact drastically the scaffold lifetime. Besides, the scaffold must progressively degrade, weaken and be replaced by the new tissue that will assume the biological function. Therefore, the control of the scaffold durability is of paramount importance since changes in mechanical, physico-chemical and morphological properties, occurring during degradation, must be at appropriate rate to avoid decreasing in the efficiency of tissue reconstruction. For instance, it has been suggested a degradation rate longer than 18 months for scaffolds dedicated to bone regeneration [2]. Since the understanding of the scaffold degradation is crucial for their successful use in tissue engineering, various *in vitro* studies have been carried out to investigate the scaffold durability through methods under physiologically or accelerated conditions with the aim to put in evidence bond cleavages, changes in chemical functionality and in mechanical properties [3–6]. However, few studies focus on approaches allowing the prediction of the scaffold lifetime [7,8]. Indeed, it is well known that it is difficult to correlate *in vitro* degradation with *in vivo* expectation since *in vivo* conditions are more complex and lead to variation of the scaffold lifetime [9,10]. Nevertheless since long-term *in vivo* degradation rate are unavailable and a human implantation strategy cannot be used to screen the durability of new scaffolds, there is a need for approaches using accelerated testing protocols to predict the lifetime of materials that are under development.

Lately, biodegradable elastomers face a growing use in tissue engineering and regenerative medicine, since they exhibit mechanical behavior that better matches the soft tissue stress–strain response and they may support reversible deformation from dynamical mechanical environments [11]. As a consequence, they allow cell migration and organization without significant irritation and lead to a reduction in foreign body response [12]. Moreover, another advantage of biodegradable elastomers lies in the possibility to tune the material thermo-mechanical properties and degradation kinetics by an appropriate selection of the synthesis and process conditions [13]. In particular, cross-linked elastomers tend to degrade advantageously with a constant three-dimensional structure, due to the combination of bulk and surface erosion, and exhibit a lowest hydrolytic degradation than the linear counterpart due to a more stable molecular structure [14,15]. The family of biodegradable elastomers includes polyurethane-based materials, the chemical composition of which ultimately affects oxidative, hydrolytic or enzymatic degradation. For instance, it is well known that poly(ether urethanes) are more stable in an aqueous environment than poly(ester urethanes) since the ester linkage is more cleavable than the urethane one. However, poly(ether ester urethanes) containing poly(ethylene glycol) fragments undergo a faster hydrolysis than poly(ester urethanes) due to a higher hydrophilicity [16]. In the frame of scaffold design, it is therefore necessary to use versatile tools allowing an easy investigation of the differences in the hydrolysis rate between materials.

In previous studies [17–19], we have developed elastomeric cross-linked poly(ester-urethane-urea) (PEUU) scaffolds through an emulsion technique allowing to produce highly interconnected porous structure used for hard and soft tissue regeneration. As a matter of fact, variation of the emulsion parameters can lead to a range of functionalities and possible applications. As an example in order to provide an appropriate surface chemistry for growth factor retention and extracellular matrix deposit, we functionalized the PEUU scaffold pore

surface with low molecular weight fucoidan (PEEUF) concomitantly to the scaffold elaboration. After 7 months of incubation at 37°C in culture medium, we did not found any variation in scaffold mass, water uptake, water contact angle or release of acidic degradation products for both PEUU and PEUUF scaffolds, despite the fact that the surface wettability of PEUUF scaffolds was slightly increased. Moreover, Attenuated Total Reflection Fourier-Transform Infrared spectroscopy (ATR-FTIR) analysis revealed a decrease of 2.7% and 2.8% of the intensity of the peak at 1158 cm^{-1} corresponding to the stretching vibrations of the ester moiety for PEUU and PEUUF scaffolds, respectively, showing the initiation of chain scissions and therefore hydrolytic degradation [18,19]. When accelerated ageing was performed at 90°C, hydrolytic degradation, which is temperature dependant, was enhanced. Indeed, the peak attributed to the ester groups decreased up to 67.2% and 71.8% after 70 days of incubation for PEUU and PEUUF scaffolds, respectively. Finally through the mass loss analysis, we estimated the lifetime at 37°C within the range of 14.2 - 46.5 months for both scaffolds. In order to refine these values and to compare both scaffolds, it is necessary to carry out a deeper investigation leading to the determination of the activation energy of the degradation process.

The aim of the present study was to predict the lifetime of cross-linked poly(ester-urethane-urea) scaffolds in culture medium at 37°C using thermally-accelerated ageing at different temperatures: 37°C, 55°C, 75°C and 90°C. Water uptake, mass loss, number average molecular weight between cross-links, water contact angle and mechanical properties were analyzed and the relation between these parameters evaluated. Compressive set measurements were also performed as an indicator of the scaffold lifetime at 90°C. Interestingly in this study, we demonstrated that the scaffold chemical composition was temperature dependant and the analysis of its variation by ATR-FTIR spectroscopy allowed an easy determination of the activation energy of the hydrolytic

degradation process leading to the prediction of the scaffold lifetime at 37°C using Arrhenius extrapolation.

2. Materials and methods

2.1 Materials

Hexamethylene diisocyanate, triol ε-caprolactone oligomers, Span®80 and dibutyltin dilaurate were purchased from Sigma-Aldrich. Dulbecco's modified Eagle's medium (DMEM), fungizone antimycotic (Fz), penicillin (Pen), and streptomycin (Strep) were supplied by Gibco Life Technologies. All solvents were purchased from Fisher and used as received.

2.2 Scaffold preparation

PEUU scaffolds were obtained by cross-linking a high internal phase emulsion (HIPE) as described previously [17]. The scaffolds were designed with a fully interconnected porosity of 85% and a multi-scale porous structure with pore sizes ranging from 50 µm to 2000 µm. Prior to use for the degradation test, the scaffolds (2 mm in thickness, 1 cm in diameter) were conditioned and sterilized through the following process: immersion in sterile water for 1 hour under a vacuum system, immersion after water change for 4 hours, immersion for 1 hour in 70 vol.% ethanol under a vacuum system, rinsing in sterile water overnight and autoclaving in wet condition.

2.3 Accelerated ageing study

The degradation assay was carried out according to ISO 10993-13 guideline standards at four temperatures: 37°C, 55°C, 75°C and 90°C. 0.1 g of PEUU scaffolds were immersed in 1 mL of degradation medium composed of DMEM/Pen (100 IU/mL)/Strep (100 µg/mL)/Fz (2.5 µg/mL),

and incubated at the desired temperature for different periods of time. The pH of the degradation medium was monitored during the course of the study. At the end of each time point, scaffolds were removed from the medium and washed extensively in distilled water. Subsequently, scaffolds were air-dried up to a constant mass.

The mass loss and remaining mass were determined from the scaffold initial mass (m_0) and their residual mass after drying (m_d) using equation (1):

$$\text{Remaining mass } (\%) = [m_d / m_0] \times 100 \qquad (1)$$

The water uptake was determined from the mass of the wet scaffolds before drying (m_w) and their residual mass after drying (m_d) using equation (2):

$$\text{Water uptake } (\%) = [(m_w - m_d) / m_d] \times 100 \qquad (2)$$

The number average molecular weight between cross-links $\bar{M}_c$ was determined as described previously through swelling measurement in toluene up to the swelling equilibrium [18]. The scaffold hydrophilicity/hydrophobicity was determined through water contact angle measurement using a Digidrop Model DS GBX apparatus and Windrop++ software. The scaffold morphology was monitored using a Keyence digital microscope VHX-6000.

Finally, scaffolds were characterized by Fourier-Transformed Infrared spectroscopy (FTIR Nicolet 380 – Thermo Scientific) in an attenuated total reflectance mode (ATR – Smart Omni Sampler) within the range 500–4000 cm^{-1} with a resolution of 4 cm^{-1}. Baseline correction and normalization was applied to scale the spectra into a similar range. The hydrolysis kinetics were evaluated through the evolution as a function of time of the ratio (A_{1164}/A_{1255}) between the absorbance intensity of the ester stretching vibrations at 1164 cm^{-1} (A_{1164}) and the absorbance intensity of a reference band at 1255 cm^{-1} associated to the –CN stretching and –NH bending of the urethane bond (A_{1255}).

2.4 Mechanical analysis of scaffolds aged at 90°C

PEUU scaffolds (18 mm in diameter, 8 mm or 16 mm in height) were totally immersed in the degradation medium composed of DMEM/Pen (100 IU/mL)/Strep (100 µg/mL)/Fz (2.5 µg/mL) and aged at 90°C up to 15 days.

The effective modulus of elasticity E_1^* was assessed by compression test in the axial direction to the foam rise (8 mm in height) with a 500 N force range, 7 mm displacement range and 5 mm/min testing speed. The stress/strain relation was computer recorded and processed using Realview 3.0 software. The effective modulus of elasticity E_1^* of the porous scaffold was obtained from the linear regression at the beginning of the stress/strain curve.

Compression set measurements were carried out based on ASTM D395 and ASTM D1056 standards to determine the scaffold ability to return to its original thickness after prolonged compressive stresses under constant deflection. PEUU scaffolds (16 mm in height) were compressed between spacer bars (thickness of t_s = 12 mm), in the axial direction to the foam rise, to 75% of its original thickness (t_0 = 16 mm) for 22 hours at room temperature. After a 30 minutes recovery period, the final thickness (t_f) was measured and the compression set (Comp. Set), expressed as a percentage of the original deflection, was calculated using equation (3):

$$\text{Comp. Set } (\%) = [(t_0 - t_f)/(t_0 - t_s)] \times 100 \qquad (3)$$

2.5 Data analysis

For measured parameters of PEUU scaffolds, values are expressed as mean ± standard deviation (SD).

3. Results and discussion

3.1 PEUU scaffold degradation

It is well known that polymeric biomaterials are subject *in vivo* to various degradation processes, in particular hydrolysis and oxidation. As a first approach to simply and straightforwardly screen the durability of biodegradable scaffolds, the present study focuses on chemical degradation due to hydrolysis mechanism through incubation in culture medium.

In the frame of evaluating lifetime of scaffolds dedicated to tissue engineering, degradation study was first performed at 37°C. At this temperature, no variation in scaffold mass (Fig. 1A), water uptake (Fig. 1B) and water contact angle (Fig. 1D) was noticed over 7 months of incubation in the degradation medium. No change of scaffold size and porous morphology was noticed over 7 months of incubation (Fig. 2B). Moreover, there was no variation of the degradation medium pH (Fig. 1C) indicating the absence of acidic degradation product release as expected for hydrolysis of PEUU scaffolds containing polyester fragments [19]. However, a small increase in the number average molecular weight between cross-links $\overline{M}_c$ was noticed from 6 months of incubation (Fig. 1E), which was attributed to the initiation of chain scissions in the cross-linked structure.

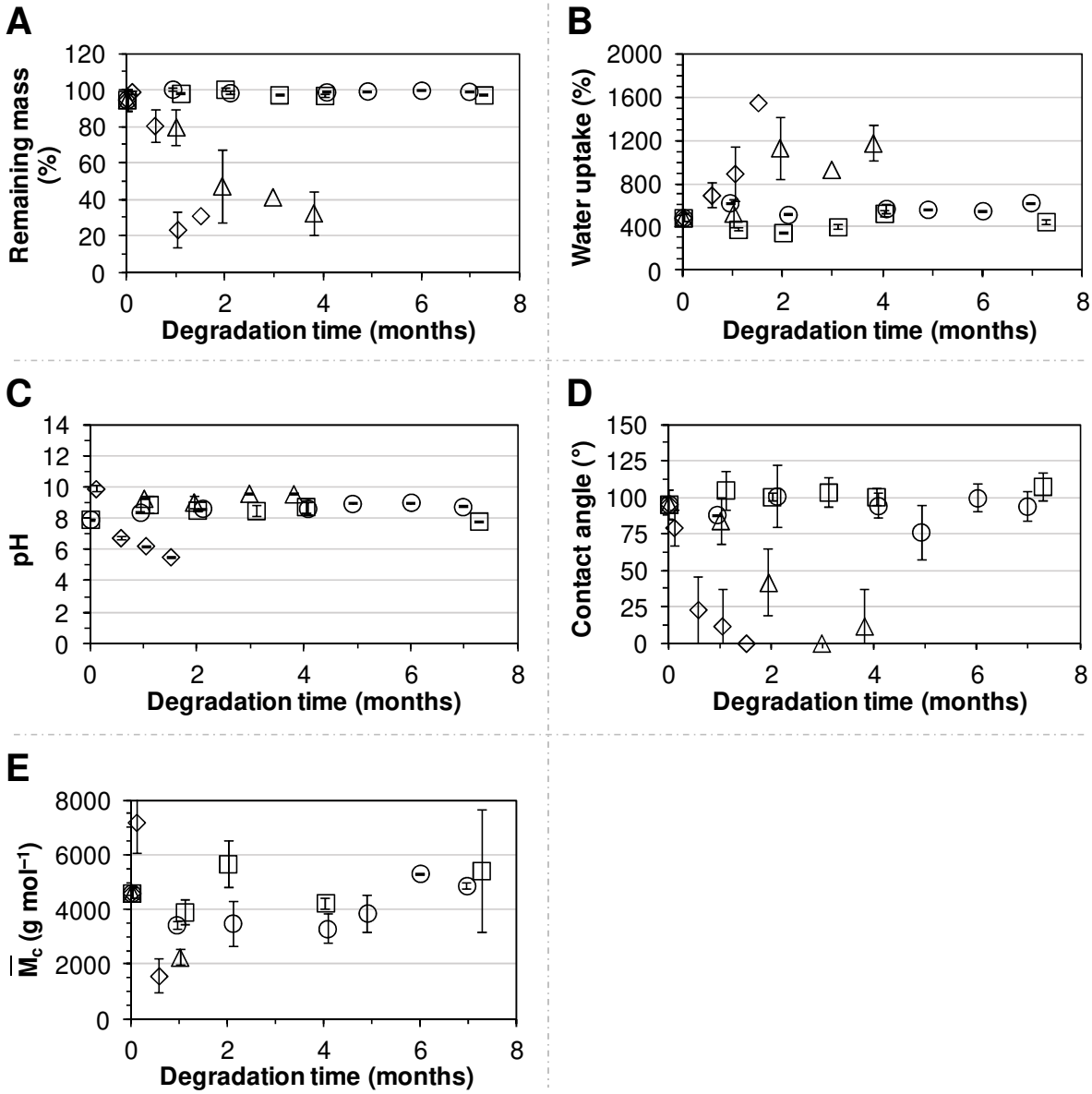

Fig. 1. Incubation of PEUU scaffolds in the degradation medium at 37°C (circle ○), 55°C (square □), 75°C (triangle Δ) and 90°C (rhombus ◊): (A) Remaining mass; (B) Water uptake; (C) pH of the degradation medium; (D) Water contact angle; (E) Number average molecular weight between cross-links $\overline{M}_c$.

Due to the slow rate of PEUU scaffold degradation at 37°C, it was necessary to perform accelerated ageing tests in order to assess the scaffold degradation within a shorter period of time. Ageing in aqueous environment is commonly accelerated using the time-temperature equivalence principle by increasing the temperature of the degradation medium. Both water diffusion and hydrolysis reaction have a temperature dependence, but hydrolysis is more impacted by temperature rising because of a higher activation energy [7]. As a consequence in the present study, we only focused on the hydrolytic degradation process and we used three other temperatures for the degradation analysis (55°C, 75°C, 90°C). As expected, the hydrolytic degradation increased with the temperature. No significant difference was found in scaffold mass, water uptake, water contact angle, degradation medium pH and number average molecular weight between cross-links $\bar{M}_c$ between degradation at 55°C and 37°C (Fig. 1). No change of scaffold size and porous morphology was noticed over 7 months of incubation at 55°C (Fig. 2C). On the other hand, drastic variations were found at 75°C and 90°C. Indeed, mass loss occurred from 3 days of incubation and reached around 70% after 3.8 months and 1.5 months of incubation at 75°C and 90°C, respectively (Fig. 1A). No change of scaffold size and porous morphology was noticed after 30 days and 13 days of incubation at 75°C and 90°C (Fig. 2D, 2F), respectively. At longer incubation times, the porous morphology was almost maintained but scaffolds became more and more brittle with loss of fragments (Fig. 2E, 2G, 2H).

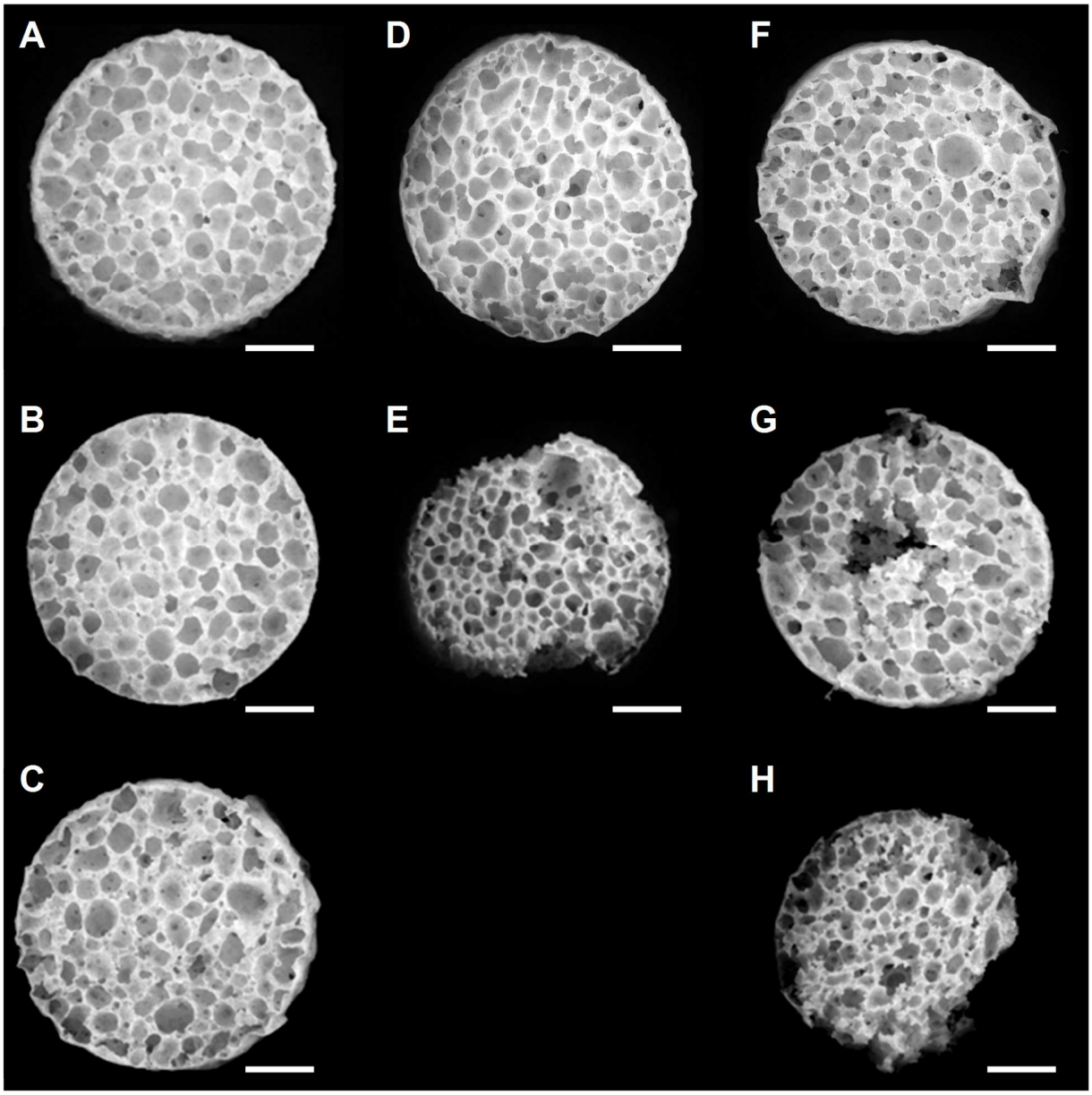

Fig. 2. Digital microscope images of PEUU scaffolds: (A) Before incubation; (B) After 209 days of incubation at 37°C in the degradation medium; (C) After 210 days of incubation at 55°C in the degradation medium; (D) After 30 days of incubation at 75°C in the degradation medium; (E) After 114 days of incubation at 75°C in the degradation medium; (F) After 13 days of incubation at 90°C in the degradation medium; (G) After 25 days of incubation at 90°C in the degradation medium; (H) After 45 days of incubation at 90°C in the degradation medium.

The FTIR analysis demonstrated that scaffold hydrolytic degradation took placed at the ester groups of PEUU scaffolds leading to the formation of carboxylic acid and hydroxyl moieties without affecting urea and urethane groups, which is in agreement with their respective stabilities [16]. Indeed, the spectrum of the PEUU scaffold before incubation presented the significant bands of poly(ester-urea-urethane)-based materials, such as urethane hydrogen-bonded –NH stretching at 3345 cm^{-1}, asymmetric and symmetric stretching of $–CH_2$ groups at 2939 and 2860 cm^{-1}, –C=O groups for urethane and ester at 1730 cm^{-1} and for urea at 1625 cm^{-1}, urea –CNH groups at 1575 cm^{-1} and urethane –NH bending at 1540 cm^{-1}, –CN stretching and –NH bending associated with urethane groups at 1255 cm^{-1}, and finally the stretching vibrations of the ester groups at 1164 cm^{-1} (Fig. 3E) [17]. The spectrum of the PEUU scaffold after 76 days of incubation at 90°C in the degradation medium presented a nearly absence of the peak of the ester groups at 1164 cm^{-1}, while the peak at 1255 cm^{-1} associated with urethane groups remained with the same intensity (Fig. 3A). Moreover, a peak associated with –C=O groups of carboxylic acid bond appeared at 1691 cm^{-1} and the intensity of the peak at 3345 cm^{-1} increased because of the formation of –OH groups. The FTIR analysis also showed the increase of hydrolytic degradation with the temperature since the peak intensity at 1164 cm^{-1} decrease by 2.7%, 10.4% and 47.7% after 209 days of incubation at 37°C (Fig. 3D), 210 days of incubation at 55°C (Fig. 3C) and 89 days of incubation at 75°C (Fig. 3B), respectively.

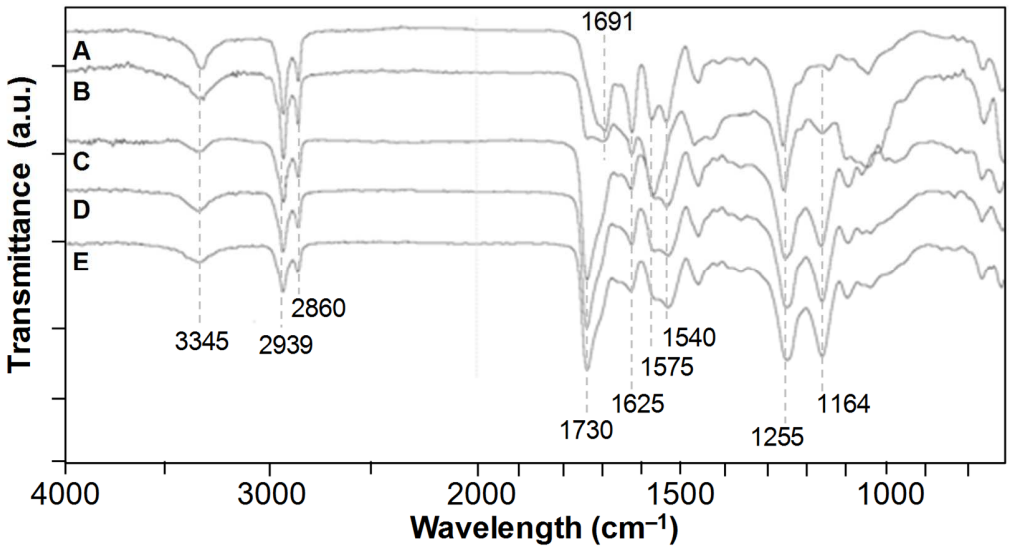

Fig. 3. ATR-FTIR spectra of PEUU scaffolds: (A) After 76 days of incubation at 90°C in the degradation medium; (B) After 89 days of incubation at 75°C in the degradation medium; (C) After 210 days of incubation at 55°C in the degradation medium; (D) After 209 days of incubation at 37°C in the degradation medium; (E) Before incubation.

The formation of carboxylic acid and hydroxyl moieties, which have a strong water affinity, led to the increase of scaffold wettability (Fig. 1D) and water uptake over degradation course (Fig. 1B). It was also noticed an increase of the number average molecular weight between cross-links $\overline{M}_c$ after 3 days of incubation at 90°C due to chain scission followed by a decrease or the impossibility to determine its value because of the scaffold brittleness (Fig. 1E). Finally, the hydrolytic degradation was associated with the release of acidic degradation products as attested by the variation of the degradation medium pH (Fig. 1C). It has to be pointed out that the variation of the degradation medium pH was not evidenced for incubation at 75°C because the medium tended to evaporate and required replenishment of the solution over the degradation course.

The change of the mechanical behavior of PEUU scaffolds was followed up through compression tests. After 10 days of incubation at 90°C in the degradation medium (Fig. 4A), the PEUU scaffold still exhibited the typical stress-strain response of an elastomeric open-cell foam. Indeed, a visco-elastic domain, characterized by a linear stress-strain relationship allowing the determination of the effective elasticity modulus E_1*, is present at the beginning of the stress-strain curve, followed by a long elastic plateau due to pore collapse and finally when all the pores have collapsed, the stress increases rapidly due to densification [20]. As expected, hydrolytic degradation and chain scissions promoted loss of mechanical properties, since the degraded scaffold exhibited lower yield stress value and effective elasticity modulus. As a matter of fact, the effective elasticity modulus decreased from the beginning of the incubation at 90°C in accordance with the variation of the cross-linking density due to chain scissions (Fig. 4B), since the number average molecular weight between cross-links $\bar{M}_c$ is inversely proportional to the effective elasticity modulus [21]. Finally, the toughness, corresponding to the area under the stress-strain curve, decreased. Indeed, the PEUU scaffold became brittle during the degradation and this embrittlement might induce pore wall rupture and collapse of the foam structure during the compression test [22]. For instance, PEUU scaffolds incubated 15 days at 90°C in the degradation medium crashed over the compression test.

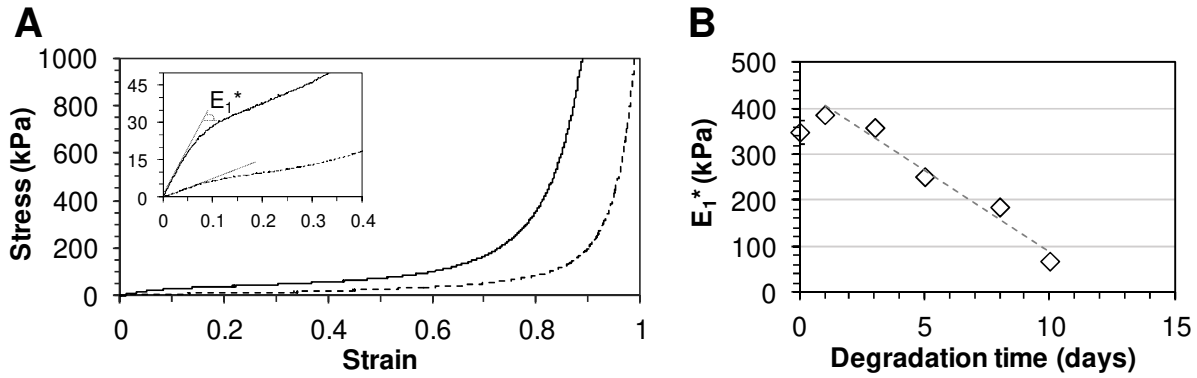

Fig. 4. (A) Mechanical behavior under stress modes of compression of PEUU scaffolds before incubation (full line) and after 10 days of incubation at 90°C in the degradation medium (dotted line); (B) Evolution of the effective modulus of elasticity E_1^* of PEUU scaffolds after incubation at 90°C in the degradation medium over a period of 10 days.

3.2 Arrhenius activation energy

Time-temperature superposition concepts and thermally-accelerated ageing tests have been widely used to predict polymer lifetime [23,24]. In most studies, Arrhenius model is used to describe the relation between the reaction rate constant *k* and the temperature by following up the variation with time of parameters, such as molar mass, hydrolysis percentage, cross-linking density, intrinsic viscosity and mechanical properties [24–31]. In the present study, the scaffold degradation was associated with the hydrolytic instability of ester groups, while urethane and urea groups remained unaffected on the time range needed to reach loss of mechanical properties, and therefore we used FTIR spectroscopy as a quantitative indicator of the hydrolysis content. The hydrolysis kinetics were evaluated through the evolution as a function of incubation time of the ratio between the absorbance intensity of the ester stretching vibrations at 1164 cm^{-1} (A_{1164}) and the absorbance intensity of the band at 1255 cm^{-1} associated to the –CN stretching and –NH

bending of the urethane bond (A_{1255}), which was chosen as reference due to relative constant intensity. This ratio is denoted A_{1164}/A_{1255}. As expected, the absorbance intensity ratio decreased with rising incubation time and temperature (Fig. 5A). The dependence of ester group cleavage on time of incubation was determined by regression analysis. The linearity of the data over time suggests that the reaction rate *k* for ester hydrolysis at a given temperature, which is proportional to the slope of the least-squared, is constant.

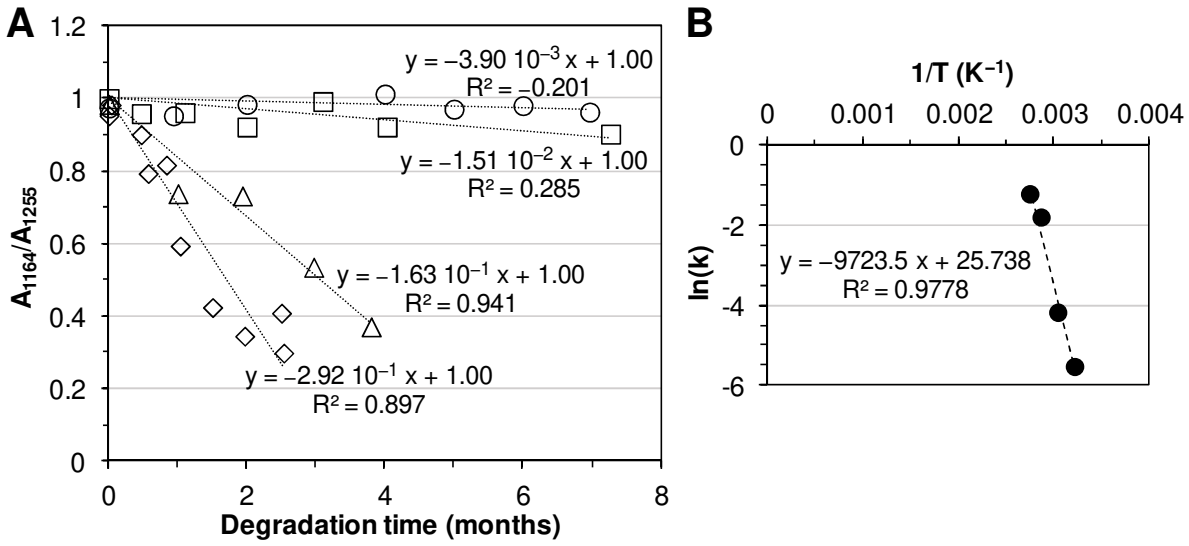

Fig. 5. (A) Evolution as a function of time of the ratio of FTIR absorbance intensities (A_{1164}/A_{1255}) of PEUU scaffolds incubated in the degradation medium at 37°C (circle ○), 55°C (square □), 75°C (triangle Δ) and 90°C (rhombus ◊) - each approximated by a linear regression curve; (B) Arrhenius plot for reaction rates derived from the linear regression of FTIR absorbance intensities as a function of time - the slope of the data in this plot is equal to $-E_a/R$.

Chaffin *et al.* [26] have demonstrated that the temperature dependence of poly(ether urethane) hydrolysis can be described by an Arrhenius analysis according to equation (4):

$$k = A\,[bond]_0[H_2O]_0 \exp[-E_a/(RT)] \qquad (4)$$

In equation 4, T is the temperature at which the degradation assay was performed, E_a is the activation energy of the degradation reaction and R is the gas constant. Since $[bond]_0$, which refers to the initial concentration of the chemical linkage that will cleave over time (in our case, ester groups), and $[H_2O]_0$, which refers to the water content in the polymer, are not strongly temperature dependent, the activation energy of the degradation reaction can be extrapolated according to equation (5):

$$\mathrm{Ln}(k + C) = -E_a/(RT) \qquad (5)$$

The combination of elevated temperature tests and Arrhenius type extrapolation is a common approach to evaluate the lifetime of many different polymeric materials over various and more or less large temperature range [32]. An important feature in accelerated ageing is the identification of the polymer system testing temperature upper limit under which the Arrhenius relation remains valid. As a matter of fact, fundamental material structure changes, such as crossing α, β and γ transitions, have to be avoid in the range of ageing temperatures used so that Arrhenius principles only reflect the chemical degradation mechanism. Indeed, activation energies are not similar when the hydrolysis reaction occurs at temperatures below and above the glass transition temperature [33]. In our study, PEUU elastomeric scaffolds are totally amorphous cross-linked systems and no transition crossing is expected in the temperature range (from 37°C to 90°C). The Arrhenius treatment was applied by plotting the logarithm of the reaction rates *k* against 1/T. Fig. 5B shows the linear evolution of the reaction rate *k* for ester hydrolysis as a function of 1/T. This linearity ($R^2 = 0.9778$) demonstrates that the data exhibit an Arrhenius behavior and that there was no change in the chemical degradation pathway in the range of temperatures used in this study, as also attested by the same evolution of FTIR spectra. As a consequence, the accelerated ageing assays can be used to predict the scaffold lifetime at 37°C since lifetime estimation by

Arrhenius extrapolation assumes that there is no change of degradation mechanism at all relevant temperatures (from 37°C to 90°C in our study) and it is suggested to carry out accelerated ageing close to the service temperature (37°C in our study) in order to valid the prediction [25,28]. From the slope of the data, we found an activation energy of the hydrolytic degradation reaction of 80.84 kJ mol^{-1}. This value is in good agreement with reported values from literature for poly(ester urethane) hydrolysis ranging from 69.5 to 83.3 kJ mol^{-1} [34,35].

3.3 PEUU scaffold lifetime prediction

In lifetime prediction, it is essential to set the critical parameter from the point of view of the scaffold functional reliability. In the field of elastomeric materials, the failure criterion could be based on the material inability to resist permanent deformation under a given deflection and to return to its original thickness. As a matter of fact, the compressive set of elastomeric material should not equal or exceed a value of 25% [36].

Fig. 6 shows the change in PEUU scaffold compression set as a function of incubation time in the degradation medium at 90°C. When the degradation time increased, PEUU scaffolds lost the ability to return to its original thickness and compressive set increased. Indeed as already perceived during compression test, hydrolytic degradation and chain scissions induced pore wall rupture when a compressive stress was applied on the degraded scaffold. Ultimately, the pore wall fracture inhibited the recovery of the original porous structure. Finally, the compressive set reached a value of 25% over a timescale of 11.6 days of incubation in the degradation medium, which set the scaffold lifetime at 90°C.

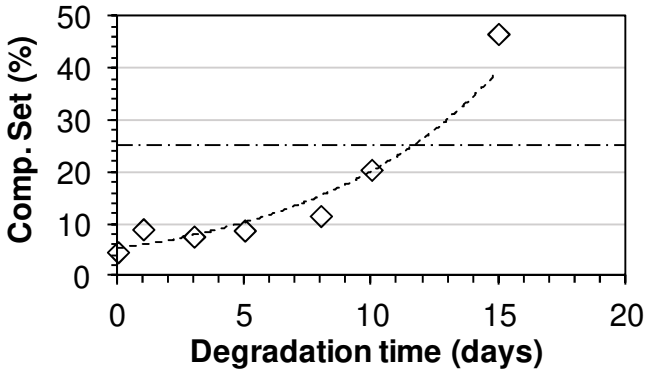

Fig. 6. Evolution of the compression set of PEUU scaffolds after incubation at 90°C in the degradation medium over a period of 15 days.

When using thermally-accelerated ageing, a common approach is to assume that the degradation rate is increased by an acceleration factor *f* corresponding to the ratio of the lifetime $t_{lifetime}$ at which to study the effects of degradation (T_{ref} = 37°C) and the lifetime t_{acc} at the elevated temperature used to accelerate the degradation process (for example T_{acc} = 90°C), as shown in equation (6):

$$f = t_{lifetime} / t_{acc} \qquad (6)$$

Using the Arrhenius model [37], the acceleration factor *f* can be calculated by equation (7):

$$f = \exp[- E_a/R \times (1/T_{acc} - 1/T_{ref})] \qquad (7)$$

In equation 7, T_{acc} is the elevated temperature used to accelerate the degradation process (for example T_{acc} = 90°C), T_{ref} is the temperature at which to study the effects of degradation (T_{ref} = 37°C), E_a is the activation energy of the degradation reaction (E_a = 80.84 kJ mol^{-1} for PEUU scaffold hydrolysis) and R is the gas constant.

As a consequence, it was possible to conclude that the PEUU scaffold lifetime of 11.6 days at 90°C led to estimate the scaffold lifetime at 37°C to 1131 days (3.1 years) using an acceleration factor *f* equal to 97.5.

Interestingly, the absorbance intensity ratio A_{1164}/A_{1255} was equal to 0.89 for PEUU scaffold incubated 11.6 days at 90°C in the degradation medium and this value could be taken as a failure criterion to predict the lifetime of new materials. As an example, we found an activation energy of the hydrolytic degradation reaction of 80.90 kJ mol^{-1} and an acceleration factor *f* of 97.8 between accelerated ageing at 90°C and the target reference of 37°C for scaffolds functionalized with low molecular weight fucoidan (PEUUF) (data not shown). The PEUUF scaffold lifetime at 90°C was found to be 10.8 days from the FTIR analysis leading to a predicted scaffold lifetime at 37°C of 1056 days. This small decrease of scaffold lifetime is in good agreement with the slight increase of PEUUF scaffold wettability due to functionalization and with the evolution with the incubation time and the degradation temperature of scaffold mass, water uptake, water contact angle, degradation medium pH and the number average molecular weight between cross-links $\overline{M}_c$.

4. Conclusions

In the present study, we investigated the thermally-accelerated ageing and lifetime prediction in culture medium of cross-linked poly(ester-urethane-urea) scaffolds. The study revealed that the scaffold chemical composition variation was temperature dependant and its analysis by FTIR spectroscopy allowed an easy determination of the activation energy of the hydrolytic degradation process leading to the prediction of the scaffold lifetime at 37°C using Arrhenius extrapolation. However, it is well established that *in vivo* conditions are complex and lead to scaffold degradation through a variety of mechanisms. For instance, polyurethane-based biomaterials are susceptible to oxidation *in vivo* which reduces its lifetime. As a consequence, it is necessary to extend the study to various degradation media to better mimic *in vivo* conditions. The approach developed in this study could be a convenient way to simply and straightforwardly

screen the durability of scaffolds when performing experimental design aiming to tailor scaffold lifetime.

Acknowledgements

The authors thank the Ministère de l'Enseignement Supérieur, de la Recherche et de l'Innovation for the MENRT scholarship granted to Credson Langueh.

CRediT authorship contribution statement

Credson Langueh: Investigation. **Sylvie Changotade**: Supervision, Resources. **Salah Ramtani**: Supervision, Resources. **Didier Lutomski**: Funding acquisition. **Géraldine Rohman**: Conceptualization, Supervision, Formal analysis, Project Administration, Writing - original draft, Writing - review & editing.

Declaration of competing interest

The authors declare that they have no conflict of interest.

References

[1] E. Sachlos, J.T. Czernuszka, Making Tissue Engineering Scaffolds Work. Review: The application of solid freeform fabrication technology to the production of tissue engineering scaffolds, Eur Cell Mater. 5 (2003) 29–40. https://doi.org/10.22203/eCM.v005a03.

[2] S.L. Cooper, J. Guan, eds., Advances in polyurethane biomaterials, Woodhead Publishing, Cambridge, 2016.

[3] C.X.F. Lam, M.M. Savalani, S.-H. Teoh, D.W. Hutmacher, Dynamics of *in vitro* polymer degradation of polycaprolactone-based scaffolds: accelerated *versus* simulated physiological conditions, Biomed Mater. 3 (2008) 034108. https://doi.org/10.1088/1748-6041/3/3/034108.

[4] L. Vikingsson, G. Gallego Ferrer, J.A. Gómez-Tejedor, J.L. Gómez Ribelles, An "*in vitro*" experimental model to predict the mechanical behavior of macroporous scaffolds implanted in articular cartilage, J Mech Behav Biomed Mater. 32 (2014) 125–131. https://doi.org/10.1016/j.jmbbm.2013.12.024.

[5] C. Zhu, S.R. Kustra, C.J. Bettinger, Photocrosslinkable biodegradable elastomers based on cinnamate-functionalized polyesters, Acta Biomater. 9 (2013) 7362–7370. https://doi.org/10.1016/j.actbio.2013.03.041.

[6] G. Guo, Q. Ma, F. Wang, B. Zhao, D. Zhang, Kinetic evaluation of the size-dependent decomposition performance of solvent-free microcellular polylactic acid foams, Chin Sci Bull. 57 (2012) 83–89. https://doi.org/10.1007/s11434-011-4873-5.

[7] D. Farrar, Modelling of the degradation process for bioresorbable polymers, in: F. Buchanan (Ed.), Degradation Rate of Bioresorbable Materials - Prediction and Evaluation, 1st edition, Woodhead Publishing, Cambridge, 2008: pp. 183–206.

[8] P. Tomlins, Influence of porous structure on bioresorbability: Tissue engineering scaffolds, in: F. Buchanan (Ed.), Degradation Rate of Bioresorbable Materials - Prediction and Evaluation, 1st edition, Woodhead Publishing, Cambridge, 2008: pp. 234–264.

[9] J.P. Santerre, K. Woodhouse, G. Laroche, R.S. Labow, Understanding the biodegradation of polyurethanes: From classical implants to tissue engineering materials, Biomaterials 26 (2005) 7457–7470. https://doi.org/10.1016/j.biomaterials.2005.05.079.

[10] J.C.Y. Chan, K. Burugapalli, J.L. Kelly, A.S. Pandit, Influence of clinical application on bioresorbability: Host response, in: F. Buchanan (Ed.), Degradation Rate of Bioresorbable

Materials - Prediction and Evaluation, 1st edition, Woodhead Publishing, Cambridge, 2008: pp. 267–318.

[11] G. Chen, T. Ushida, T. Tateishi, Hybrid biomaterials for tissue engineering: A preparative method for PLA or PLGA–collagen hybrid sponges, Adv Mater. 12 (2000) 455–457. https://doi.org/10.1002/(SICI)1521-4095(200003)12:6<455::AID-ADMA455>3.0.CO;2-C.

[12] M. Montgomery, L. Davenport Huyer, D. Bannerman, M.H. Mohammadi, G. Conant, M. Radisic, Method for the fabrication of elastomeric polyester scaffolds for tissue engineering and minimally invasive delivery, ACS Biomater Sci Eng. 4 (2018) 3691–3703. https://doi.org/10.1021/acsbiomaterials.7b01017.

[13] C.J. Bettinger, Biodegradable elastomers for tissue engineering and cell-biomaterial interactions, Macromol Biosci. 11 (2011) 467–482. https://doi.org/10.1002/mabi.201000397.

[14] S. Rupnik, S. Buwalda, S. Dejean, A. Bethry, X. Garric, J. Coudane, B. Nottelet, Redox reducible and hydrolytically degradable PEG-PLA elastomers as biomaterial for temporary drug-eluting medical devices, Macromol Biosci. 16 (2016) 1792–1802. https://doi.org/10.1002/mabi.201600132.

[15] A. Pegoretti, L. Fambri, A. Penati, J. Kolarik, Hydrolytic resistance of model poly(ether urethane ureas) and poly(ester urethane ureas), J Appl Polym Sci. 70 (1998) 577–586. https://doi.org/10.1002/(SICI)1097-4628(19981017)70:3<577::AID-APP20>3.0.CO;2-X.

[16] X. Zhang, K.G. Battiston, J.E. McBane, L.A. Matheson, R.S. Labow, J.P. Santerre, Design of biodegradable polyurethanes and the interactions of the polymers and their degradation by-products within *in vitro* and *in vivo* environments, in: S.L. Cooper, J. Guan (Eds.), Advances in Polyurethane Biomaterials, Woodhead Publishing, Cambridge, 2016: pp. 75–114. https://doi.org/10.1016/B978-0-08-100614-6.00003-2.

[17] S. Changotade, G. Radu Bostan, A. Consalus, F. Poirier, J. Peltzer, J.-J. Lataillade, D. Lutomski, G. Rohman, Preliminary *in vitro* assessment of stem cell compatibility with cross-linked poly(ε-caprolactone urethane) scaffolds designed through high internal phase emulsions, Stem Cells Int. 2015 (2015) 283796. https://doi.org/10.1155/2015/283796.

[18] G. Rohman, S. Changotade, S. Frasca, S. Ramtani, A. Consalus, C. Langueh, J.-M. Collombet, D. Lutomski, *In vitro* and *in vivo* proves of concept for the use of a chemically cross-linked poly(ester-urethane-urea) scaffold as an easy handling elastomeric biomaterial for bone regeneration, Regen Biomater. (2019). https://doi.org/10.1093/rb/rbz020.

[19] G. Rohman, C. Langueh, S. Ramtani, J.-J. Lataillade, D. Lutomski, K. Senni, S. Changotade, The use of platelet-rich plasma to promote cell recruitment into low-molecular-weight fucoidan-functionalized poly(ester-urea-urethane) scaffolds for soft-tissue engineering, Polymers 11 (2019) 1016. https://doi.org/10.3390/polym11061016.

[20] G. Ben-Dor, G. Mazor, G. Cederbaum, O. Igra, Stress-strain relations for elastomeric foams in uni-, bi- and tri-axial compression modes, Arch Appl Mech. 66 (1996) 409–418. https://doi.org/10.1007/BF00803675.

[21] J. Yang, A.R. Webb, S.J. Pickerill, G. Hageman, G.A. Ameer, Synthesis and evaluation of poly(diol citrate) biodegradable elastomers, Biomaterials 27 (2006) 1889–1898. https://doi.org/10.1016/j.biomaterials.2005.05.106.

[22] E. Pellizzi, A. Lattuati-Derieux, B. Lavédrine, H. Cheradame, Degradation of polyurethane ester foam artifacts: Chemical properties, mechanical properties and comparison between accelerated and natural degradation, Polym Degrad Stab. 107 (2014) 255–261. https://doi.org/10.1016/j.polymdegradstab.2013.12.018.

[23] A. Chamas, H. Moon, J. Zheng, Y. Qiu, T. Tabassum, J.H. Jang, M. Abu-Omar, S.L. Scott, S. Suh, Degradation rates of plastics in the environment, ACS Sustainable Chem Eng. 8 (2020) 3494–3511. https://doi.org/10.1021/acssuschemeng.9b06635.

[24] B. Laycock, M. Nikolić, J.M. Colwell, E. Gauthier, P. Halley, S. Bottle, G. George, Lifetime prediction of biodegradable polymers, Prog Polym Sci. 71 (2017) 144–189. https://doi.org/10.1016/j.progpolymsci.2017.02.004.

[25] P.Y. Le Gac, D. Choqueuse, D. Melot, Description and modeling of polyurethane hydrolysis used as thermal insulation in oil offshore conditions, Polym Test. 32 (2013) 1588–1593. https://doi.org/10.1016/j.polymertesting.2013.10.009.

[26] K.A. Chaffin, X. Chen, L. McNamara, F.S. Bates, M.A. Hillmyer, Polyether urethane hydrolytic stability after exposure to deoxygenated water, Macromolecules 47 (2014) 5220–5226. https://doi.org/10.1021/ma500904d.

[27] L. Fambri, A. Penati, J. Kolarik, Synthesis and hydrolytic stability of model poly(ester urethane ureas), Angew Makromol Chemie 228 (1995) 201–219. https://doi.org/10.1002/apmc.1995.052280116.

[28] K.T. Gillen, R. Bernstein, M. Celina, The challenges of accelerated aging techniques for elastomer lifetime predictions – Part 1, RFP. 1 (2017) 250–257.

[29] B. Moon, N. Jun, S. Park, C.-S. Seok, U. Hong, A Study on the modified Arrhenius equation using the oxygen permeation block model of crosslink structure, Polymers 11 (2019) 136. https://doi.org/10.3390/polym11010136.

[30] R. Bernstein, D.K. Derzon, K.T. Gillen, Nylon 6.6 accelerated aging studies: Thermal–oxidative degradation and its interaction with hydrolysis, Polym Degrad Stab. 88 (2005) 480–488. https://doi.org/10.1016/j.polymdegradstab.2004.11.020.

[31] M. Deroiné, A. Le Duigou, Y.-M. Corre, P.-Y. Le Gac, P. Davies, G. César, S. Bruzaud, Accelerated ageing and lifetime prediction of poly(3-hydroxybutyrate-co-3-hydroxyvalerate) in distilled water, Polym Test. 39 (2014) 70–78. https://doi.org/10.1016/j.polymertesting.2014.07.018.

[32] A. Plota, A. Masek, Lifetime prediction methods for degradable polymeric materials—A short review, Materials. 13 (2020) 4507. https://doi.org/10.3390/ma13204507.

[33] X. Han, J. Pan, F. Buchanan, N. Weir, D. Farrar, Analysis of degradation data of poly(L-lactide–co-L,D-lactide) and poly(L-lactide) obtained at elevated and physiological temperatures using mathematical models, Acta Biomater. 6 (2010) 3882–3889. https://doi.org/10.1016/j.actbio.2010.05.015.

[34] D.W. Brown, R.E. Lowry, L.E. Smith, Kinetics of hydrolytic aging of polyester urethane elastomers, Macromolecules 13 (1980) 248–252. https://doi.org/10.1021/ma60074a009.

[35] L. Fambri, A. Pegoretti, J. Kolarik, C. Gavazza, A. Penati, Thermal stabilities of different poyurethanes after hydrolytic treatment, J Therm Anal Calorim. 52 (1998) 789–797. https://doi.org/10.1023/A:1010118808415.

[36] M. Patel, A.R. Skinner, Thermal ageing studies on room-temperature vulcanised polysiloxane rubbers, Polym Degrad Stab. 73 (2001) 399–402. https://doi.org/10.1016/S0141-3910(01)00118-5.

[37] A. Mahomed, Ageing processes of biomedical polymers in the body, in: M. Jenkins, A. Stamboulis (Eds.), Durability and Reliability of Medical Polymers, Woodhead Publishing, Cambridge, 2012: pp. 164–182. https://doi.org/10.1533/9780857096517.2.164.

Figure captions

Fig. 1. Incubation of PEUU scaffolds in the degradation medium at 37°C (circle ○), 55°C (square □), 75°C (triangle Δ) and 90°C (rhombus ◊): (A) Remaining mass; (B) Water uptake; (C) pH of the degradation medium; (D) Water contact angle; (E) Number average molecular weight between cross-links $\overline{M}_c$.

Fig. 2. Digital microscope images of PEUU scaffolds: (A) Before incubation; (B) After 209 days of incubation at 37°C in the degradation medium; (C) After 210 days of incubation at 55°C in the degradation medium; (D) After 30 days of incubation at 75°C in the degradation medium; (E) After 114 days of incubation at 75°C in the degradation medium; (F) After 13 days of incubation at 90°C in the degradation medium; (G) After 25 days of incubation at 90°C in the degradation medium; (H) After 45 days of incubation at 90°C in the degradation medium.

Fig. 3. ATR-FTIR spectra of PEUU scaffolds: (A) After 76 days of incubation at 90°C in the degradation medium; (B) After 89 days of incubation at 75°C in the degradation medium; (C) After 210 days of incubation at 55°C in the degradation medium; (D) After 209 days of incubation at 37°C in the degradation medium; (E) Before incubation.

Fig. 4. (A) Mechanical behavior under stress modes of compression of PEUU scaffolds before incubation (full line) and after 10 days of incubation at 90°C in the degradation medium (dotted line); (B) Evolution of the effective modulus of elasticity E_l^* of PEUU scaffolds after incubation at 90°C in the degradation medium over a period of 10 days.

Fig. 5. (A) Evolution as a function of time of the ratio of FTIR absorbance intensities (A_{1164}/A_{1255}) of PEUU scaffolds incubated in the degradation medium at 37°C (circle ○), 55°C (square □), 75°C (triangle Δ) and 90°C (rhombus ◊) - each approximated by a linear regression curve; (B) Arrhenius plot for reaction rates derived from the linear regression of FTIR absorbance intensities as a function of time - the slope of the data in this plot is equal to $-E_a/R$.

Fig. 6. Evolution of the compression set of PEUU scaffolds after incubation at 90°C in the degradation medium over a period of 15 days.